

PACS №: 84.60.-h; 84.70.+p

Andreas A. Neuber, Juan-Carlos Hernandez,
James C. Dickens, Magne Kristiansen
Center for Pulsed Power and Power Electronics Research
Departments of Electrical & Computer Engineering and Physics
Texas Tech University
Lubbock, TX 79409-3102
email: andreas.neuber@ttu.edu

Helical MFCG for Driving a High Inductance Load¹

Contents

| | |
|-----------------------------------|------------|
| 1. Introduction | 397 |
| 2. Experimental Setup | 399 |
| 2.1. The Staged MFCG | 399 |
| 3. Results and Discussion | 400 |
| 3.1. Single Stage Tests | 400 |
| 3.2. Dual Stage Tests | 403 |
| 4. Conclusion | 403 |

Abstract

Even at small dimensions of less than 0.5 meter in length end-initiated helical magnetic flux compression generators (MFCG) have at least one order of magnitude higher energy density (by weight or volume) than capacitive energy storage with similar discharge time characteristics. However, simple MFCGs with a single helix produce high output energy only into low inductance loads, thus producing several 100 kA of current at a voltage level of less than 10 kV. Many pulsed power devices require less current but a considerably higher voltage level. For effectively driving a high inductance load of several μH , a multistage MFCG design has been suggested. We successfully tested a dual stage MFCG with a total length of 250 mm, a helix inner diameter of 51 mm, which is wound with Teflon insulated stranded wire of different sizes in the range from AWG 12 to AWG 22. We have presently achieved an energy gain of ~ 13 into a 3 μH load and will discuss the generator performance based on experimental current/voltage waveforms and specify the observed losses.

1. Introduction

It is well known that the experimentally observed gain of a single stage magnetic flux compression generator can be expressed as a function of the ratio of initial, L_0 , to final inductance, L_F .

$$G_I = (L_0/L_F)^\beta \quad \text{or} \quad G_E = (L_0/L_F)^{2\beta-1} \quad (1)$$

with the overall current gain, G_I , and the energy gain, G_E , respectively. The figure of merit, β , becomes unity for the ideal loss-less case, and ranges between 0.6 and

0.8 for real generators. In general, larger generators exhibit a larger β . This means that a generator with larger physical dimensions will perform superior to a smaller generator with the same L_0, L_F [1].

Typical values for L_0 range somewhere between a few tens to a few 100's μH , so that $G_E \sim 4$ or smaller for generators with less than 100 mm diameter having a final (or load) inductance, L_F , of at least 3 μH (we have used $\beta = 0.7$ in Eq. 1). Lowering the load inductance, L_F , to 100 nH will push the energy gain to ~ 40 . However, such a small load inductance is not very practical and forbids driving a variety of pulsed power loads. Obviously some kind of transformer can be used to remedy this situation.

Hence, it was suggested to combine two MFCG

¹This work was solely funded by the Explosive-Driven Power Generation MURI program funded by the Director of Defense Research & Engineering (DDR&E) and managed by the Air Force Office of Scientific Research (AFOSR).

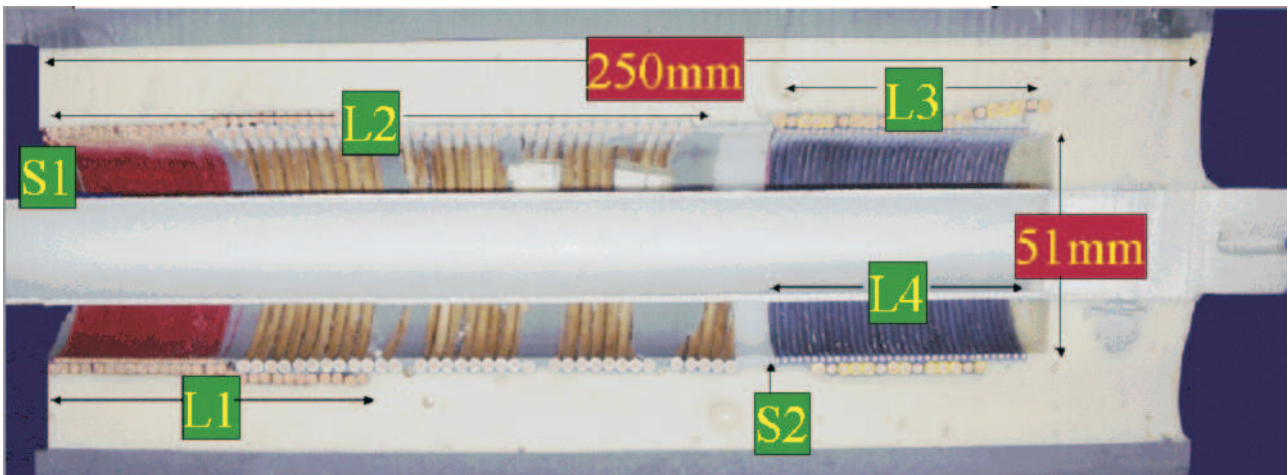
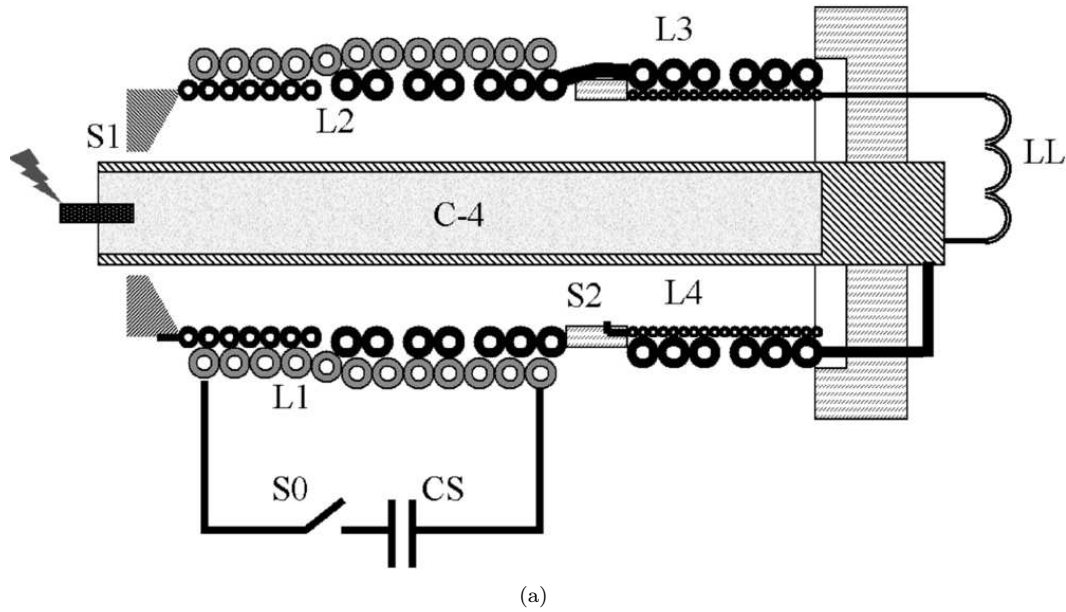


Fig. 1. Staged MFCG connected to an inductive load, LL. Storage capacitor ($50 \mu\text{F}$) – CS, Closing switch – S0, field coil for first stage – L1, Crowbar for L2 – S1, first stage coil – L2, primary of dynamic transformer – L3, Crowbar for L4 – S2, secondary of dynamic transformer – L4. See Table 1 for specific helix dimensions.

stages, the first one having a small load inductance, thus a large energy gain, and the second stage having a large final load inductance, effectively stepping up the voltage level of the first stage as it is necessary for pushing a large current in a limited amount of time into the inductive load. The key to this approach is that the load inductance of the first stage is used as the field coil for the second stage. Hence, the flux produced by the first stage is effectively trapped by the second stage.

When comparing a dynamic transformer (flux trapping) with a conventional transformer, it was found that the latter produces somewhat higher energy gain [2]. However, the former requires a smaller number of components and isolates the load from current-flow until the second stage operates.

Most documented two-stage MFCGs have been

rather large, however, a two-stage generator with 60 mm constant diameter was reported to produce an energy gain of 10 (4.5 kJ) [3]. A larger variant with 100 mm diameter first stage and tapered second stage produced a gain of 11.9 (2.8 kJ) at a higher efficiency. The limiting factor is the insulation thickness of ~ 0.5 mm for a hold-off voltage of about 50 kV between the helices, thus reducing the effective coupling coefficient between the coils.

It was also experimentally found that the second stage by itself has a higher efficiency compared to series operation with the first stage. A reduction of 50 % in efficiency due to the mutual inductance between the first and second stage is believed to be the reason for this smaller efficiency [3].

We will describe the mechanical design and the operation of a small staged system utilizing flux

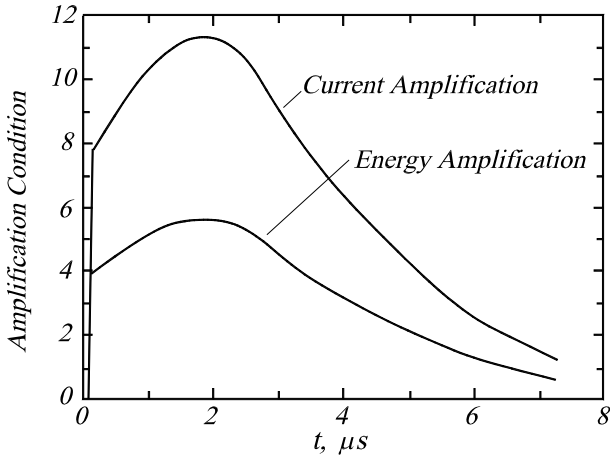


Fig. 2. Energy and current amplification condition plot for L4 using the crowbar pin configuration. Upper curve – Current amplification, see Equation (4); bottom curve – Energy amplification, see Equation (5).

trapping, with 51 mm helix diameter, 250 mm length, and a standard 3 μH load inductance.

Two different dynamic transformer configurations, crowbar disk and pin, have been tested in combination with the first stage and by itself, with the crowbar pin configuration showing a better performance when it is used in combination with the first stage.

Intrinsic and ohmic flux losses as well as the energy and current amplification have been quantified separately to determine the cause of the different performances, showing a notable difference between them.

2. Experimental Setup

2.1. The Staged MFCG

The smallest wire pitch used for the staged MFCG was set to 1.25 mm. Following the relationship between the armature's expansion angle, θ , and the pitch, p ,

$$\Delta a = \frac{p}{4} \tan \theta, \quad (2)$$

partial turn-skipping can be avoided [4] if the armature is round and centered with respect to the helix within $\Delta a \sim 0.08$ mm. We consider this required level of accuracy as only moderate so that we could utilize the manufacturing methods previously applied to our single stage, single pitch generators, which we primarily studied to gain insight in the basic physics of these generators [1]. In brief, the helices L2, L4 followed by L1 and L3, see Fig. 1, are wound on a mandrel and held in place by thin layers of epoxy. We paid specific attention to the layer between two helices, so that air voids were almost completely

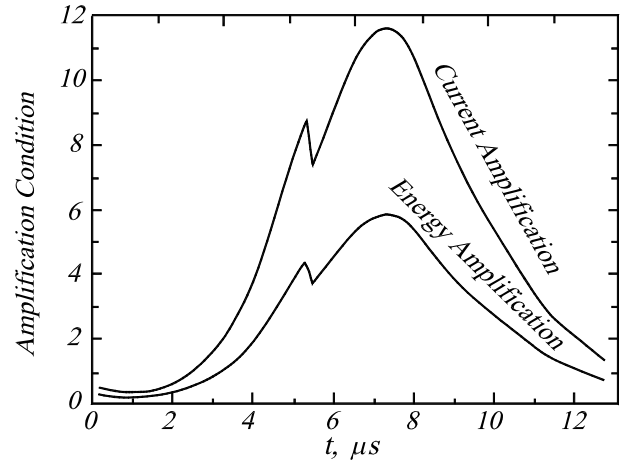


Fig. 3. Energy and current amplification condition for L4 using the crowbar disk. Upper curve – Current amplification, see Equation (4); bottom curve – Energy amplification, Equation (5).

avoided.

Before removing the mandrel, we added mechanical strength to the MFCG by inserting the generator into a PVC pipe and casting the space between generator and pipe with epoxy (overall thickness of outer layer ~ 25 mm). The seamless aluminum armature, 25 mm diameter, 2 mm wall, was partially annealed, thus ensuring proper expansion up to the helix diameter of 51 mm.

We chose the initial generator pitch as small as reasonably possible in order achieve a sufficiently large dL/dt to overcome the initially large resistance, $R(t)$ of the generator. Starting with the lumped circuit equation for the MFCG,

$$L(t) \frac{dI(t)}{dt} + \alpha \cdot I(t) \cdot \frac{dL(t)}{dt} + I(t) \cdot R(t) = 0 \quad (3)$$

it can be easily derived that

$$\alpha \cdot \left| \frac{dL(t)}{dt} \right| / R(t) > 1, \quad (4)$$

to have an instantaneous current gain > 0 , cf. Fig. 2. The parameter α describes the intrinsic flux loss and has a typical value of ~ 0.8 for our small generators ($0 < \alpha \leq 1$, $\alpha = 1$ means no intrinsic loss). Or even more restricting, for an instantaneous energy gain > 0 the following has to be true, cf. Fig. 3:

$$(2\alpha - 1) \cdot \left| \frac{dL(t)}{dt} \right| / 2R(t) > 1. \quad (5)$$

Two variants of the final stage were tested, one with a simple, Teflon-insulated pin as crowbar, S2 as shown in Fig. 1, and another with a crowbar made of a ~ 0.2 mm thin disk with a central hole diameter about 4 mm larger than the armature diameter. Additionally, the disk had a single radial slot for

Table 1. MFCG helix dimensions and inductances

| # | Wire | # turns | inductance |
|----|-----------------|------------|---------------|
| L1 | AWG 14, formvar | 15 | 10 μ H |
| L2 | AWG 22 | 40 | 52 μ H |
| | 2 x AWG12 | 6 | |
| | 3 x AWG12 | 3 | |
| | 4 x AWG12 | 2 | |
| | 5 x AWG12 | 1 | |
| L3 | 7 x AWG12 | \sim 2.5 | \sim 300 nH |
| L4 | AWG20 | 32 | 29 μ H |
| LL | AWG12 | \sim 9 | 3 μ H |

avoiding induced eddy currents in the disk. We had successfully used this type of crowbar in numerous previous experiments with our single stage generators [5] and we used the same approach for the input crowbar, S1, cf. Fig. 1. The load inductance for the second stage was fixed at 3 μ H for all shots.

The conditions for current and energy multiplication of the output stage are met during the entire operation of the output stage, L4, with crowbar pin configuration, see Fig. 2. Replacing the pin with a crowbar disk causes the amplification condition to drop below unity for the first 2 to 3 μ s, thus more energy is dissipated than produced during this early phase, see Fig. 3. Meaning, that from this point of view the crowbar disk geometry should exhibit poorer performance. The average dL/dt of helix L2 is \sim 8 Ω , which is distinctly larger than the wire resistance of initially \sim 1 Ω (resistance measured at 100 kHz frequency). The helix L1 is wound with AWG 14 magnet wire; all other helices are standard Teflon insulated copper wire (all wires off-the-shelf).

We used stranded AWG 12 for the ease of winding the wire onto the mandrel (the smaller wires were solid). No grooves were machined into the mandrel and the correct pitch was adjusted utilizing custom gages. Standard etchant was applied to the Teflon insulated wires before winding the helices, and the simple solder joints between the helices were insulated with Teflon tape and shrink tubing.

The 3 μ H load inductance was wound on a non-magnetic core and placed about 150 mm away from the generator's output end.

3. Results and Discussion

3.1. Single Stage Tests

The experimental behavior of the first and second

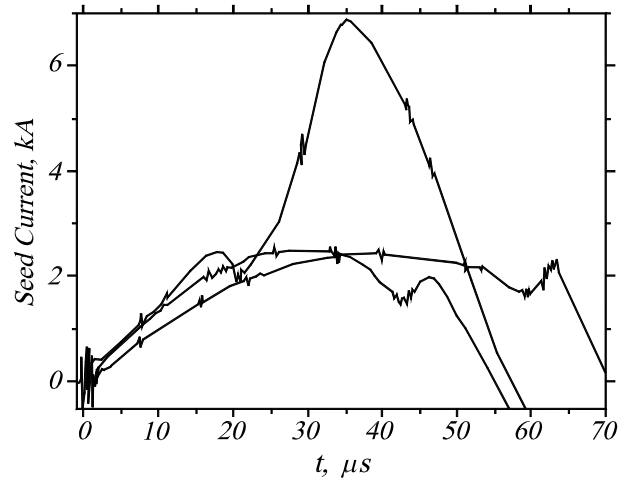


Fig. 4. Seed current for L1 extending solely over the first 40 turns of L2 (two lower curves) and covering all of L2 (upper curve).

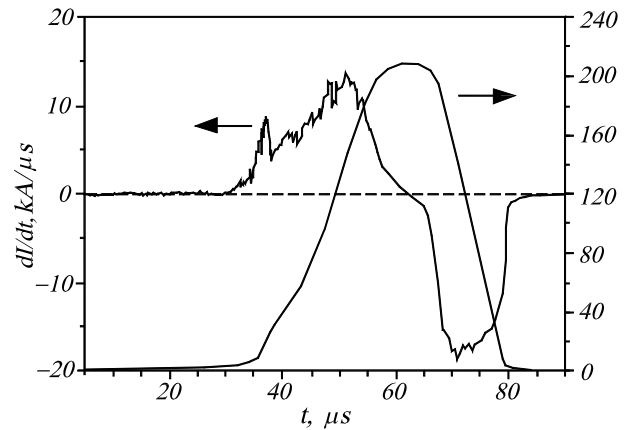


Fig. 5. dI/dt and current output of the first stage only, L2. Seed current was 12.8 kA and the energy gain was 20.

stage was observed separately by capacitor seeding either one of them without the other attached. These experiments revealed that the most efficient helix configuration for the first stage is achieved by limiting the helix length of field coil L1 to the first 40 x AWG 22 turns of L2. This ensures that L1 forms a voltage step-up transformer with L2. If L1 is chosen to span the entire length of L2, a significant amount of energy is pushed back into the capacitor seed current circuit, see upper curve in Figure 4. The output load for the first stage test was set to 350 nH, which is close to the inductance of field coil L3.

The first stage by itself produced an energy gain of 20 when seeded with \sim 13 kA. (7.8 kJ output energy).

It should be noted that we decreased the roughly 400 J seed energy to \sim 100 J for the staged MFCG shots as the induced voltage in the second stage at the high energy level could reach 100 kV or more, surely causing breakdown of the insulation. Generally, the

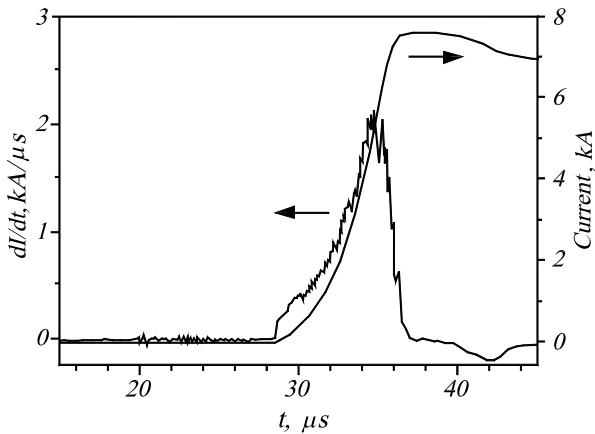


Fig. 6. dI/dt and current output for the second stage only with crowbar pin. Seed current was 20 kA into the field coil $L3 = 200$ nH and the energy gain was 0.9.

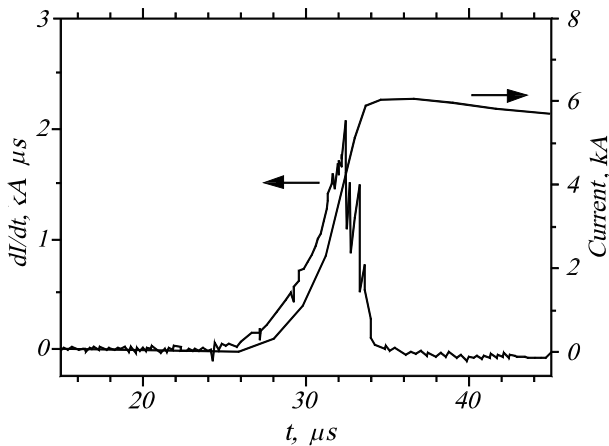


Fig. 7. dI/dt and current output for the second stage only with crowbar disk. Seed current was 19 kA into the filed coil $L3 = 200$ nH and the energy gain was 0.6.

simple solder joints utilized for joining the wires with varying pitch as well as L2 and L3 are operating close to flawless, see Figure 5.

The sharp drop in dI/dt at about $38 \mu\text{s}$ signals the moment when the armature has wiped out the first 40 turns (AWG 22) of the helix L2. About $12 \mu\text{s}$ earlier, the armature is contacting the crowbar, S1, the flux established by L1 is trapped by L2, and dI/dt exhibits a distinct positive slope when the first turns of L2 are wiped out. After about $28 \mu\text{s}$ of total runtime (at $t \sim 61 \mu\text{s}$ in Fig. 5), the first stage is burned and dI/dt goes negative.

Comparing the performance of the two geometries of the second stage, with crowbar pin, see Figure 6, and with crowbar disk, see Figure 7, reveals the inferior performance of the crowbar disk design with a 30 % smaller energy gain.

Starting with the fundamental circuit equation for

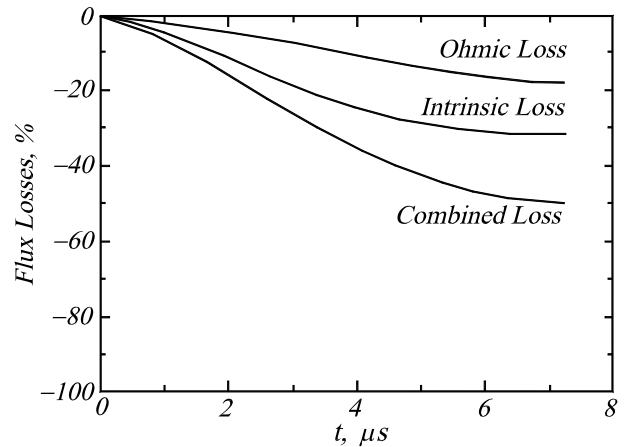


Fig. 8. Flux loss for the second stage MFCG into a $3 \mu\text{H}$ load with crowbar pin. The crowbar pin connects the second stage with the armature at the first turn at $0 \mu\text{s}$.

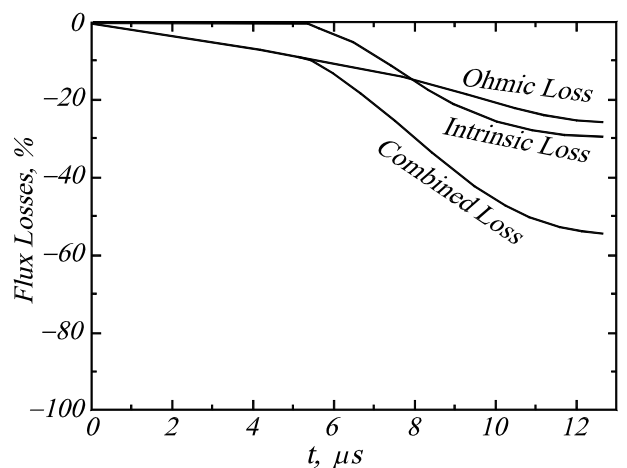


Fig. 9. Flux loss for the second stage into a $3 \mu\text{H}$ load with crowbar disk. The armature takes $\sim 5.4 \mu\text{s}$ to expand from initial crowbar to the first turn.

the second stage, we quantified the contributions of intrinsic and ohmic flux losses to the combined loss [6], see Figs. 8 and 9. This approach requires as input the time-dependent inductance, $L(t)$, and resistance, $R(t)$, which we calculated using a 3D eddy current solver accounting for magnetic field diffusion and proximity effects.

Approximately 10 % of flux is lost due to ohmic heating at the time of contact with the first turn of the crowbar disk design, Figure 9, compared to the crowbar pin, that has no losses at the same point, $0 \mu\text{s}$ in Figure 8, ending with 26 % and 18 % of flux lost due to ohmic heating, respectively at $12.7 \mu\text{s}$ and $7.3 \mu\text{s}$.

Since crowbar disk and pin have the same $L(t)$ and $R(t)$ starting from the first helix turn to the end, the intrinsic flux losses have shown to be very similar in both cases with 29 % and 31 % lost respectively,

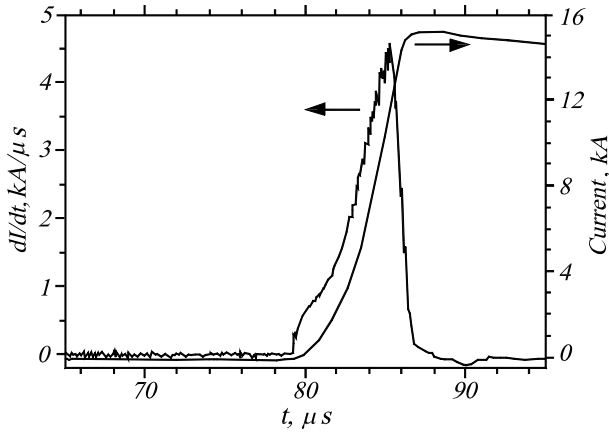


Fig. 10. dI/dt and current output for the complete 2 stage MFCG into a $3 \mu\text{H}$ load. Seed current was 2.5 kA and the overall energy gain was 13.

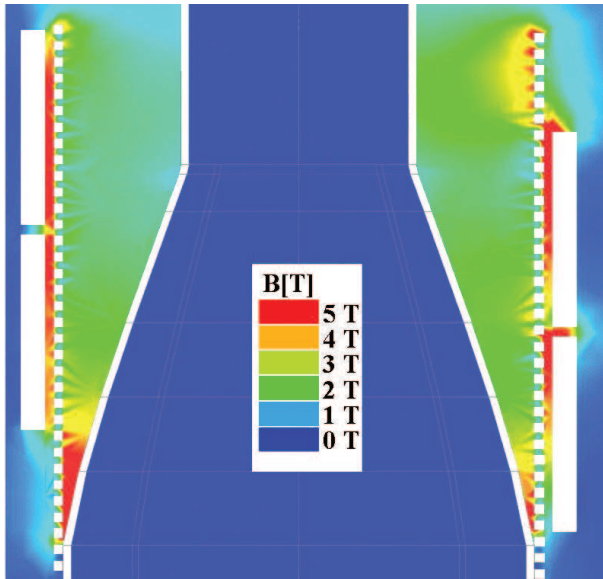


Fig. 11. Magnetic flux density at 100 kHz with 10kA current. The 34 boxes at each side represent the secondary. Two boxes with 2.5 turns represent the primary.

Figures 8 and 9, since the intrinsic losses should be small up until the armature contacts the first coil turn [6].

Nevertheless, the experimental performance for the two geometries differs more than we can explain with our simple calculations. We believe that the reason for this is the heavy insulation of the crowbar disk as it is necessary to prevent early breakdown between crowbar and armature. Some of the energy will be lost into breaking down the insulation as the armature is sliding along the insulated crowbar disk. It should be noted that the secondary winding L4 of the voltage step-up transformer formed by L3–L4 is open circuited before crowbar, thus generating a high voltage stress between the crowbar and the armature.

As desired, the energy gain, G_E , of the first stage is relatively large, whereas stage 2 serves as voltage step-up with $G_E \sim 1$. The calculated β in the secondary was 0.670 and 0.675 for crowbar disk and pin respectively, which is as expected larger than 0.5 since we have to compensate for approximately 30 % coupling losses between L3 and L4. While the first stage behaves more like a conventional MFCG with high current and energy gains, the second stage exhibits small current amplifications of ~ 5 and comparatively small experimental flux losses of $\sim 50 \%$, mainly due to the large load inductance driven. The effect of the large load, $3 \mu\text{H}$, connected to stage 2 is manifested in the current waveforms outputs in Figures 6, 7 and 10, which exhibits a large L/R time constant after generator burn. In contrast, stage 1 in Figure 5 shows a much smaller L/R constant (faster current decay), with the 300 nH load, which corresponds to the field coil L3 of the stage 2.

The crowbar pin configuration shown in Figure 2 has the disadvantage that at time $0 \mu\text{s}$ the secondary winding has already lost $\sim 40 \%$ of its volume for compression. Thus, as can be seen in equation (1), the potential current and energy amplification is relatively lower than the crowbar disk design since the initial inductance is 75 % smaller than the crowbar disk at the switching time $0 \mu\text{s}$. Figure 3 shows an abrupt drop in current and energy amplification at $5.4 \mu\text{s}$ when the crowbar disk design is used. This drop is not visible in Figure 2 with crowbar pin, since the armature makes contact to the first turn at $t = 0 \mu\text{s}$. Only at the moment of contact between armature and first turn, the flux loss parameter is assumed to drop from a $\alpha = 1$ (no intrinsic loss) to $\alpha \sim 0.8$, see Eq. 1, thus accounting for the increased flux loss throughout armature-helix contact. In addition, for the crowbar disk neither the current nor the energy is amplified in the first $2.6 \mu\text{s}$ and $3.2 \mu\text{s}$ respectively until the conditions for amplification from equations (2) and (3) are met.

The same problem arises in the first stage, which was hence designed with a high initial inductance and small pitch, 40 x AWG 22 turns of L2, to achieve a high dL/dt even during the beginnings of generator operation. After these initial 40 turns, the pitch is increased to maintain the current density and avoid excessive induced voltages throughout the compression time that might lead to breakdown.

One more disadvantage for using a crowbar disk as S2, cf. Fig. 1, is that the staged MFCG becomes physically longer and more difficult to align. Most of the generators using the crowbar disk configuration have shown clocking problems due to misalignment, exhibiting inferior performance compared to the crowbar pin design. We chose the crowbar pin for our most successful staged MFCG design, a decision that was primarily based on the lower gain and the overall higher complexity of the second stage crowbar disk.

3.2. Dual Stage Tests

Based on the performance of the two stages separately, one might expect the overall energy gain of the complete generator being close to the product of the individual gains ~ 18 . However, we consider this as the maximum gain, since, as mentioned earlier, coupling due to the mutual inductance between stages can cause a smaller, 50 %, overall gain [3]. Hence, the energy gain for the staged MFCG was expected to be in the range from 9 to 18. We observed experimentally an energy gain of 13 for the complete staged generator, see Figure 10, which is only about 30 % lower than the maximum expected gain. The only change from the single stage tests was the ~ 0.1 mm thicker Teflon insulation of the helix L3 that became necessary to avoid breakdown between the helices as well as between helix and armature at higher voltage levels (In the single-stage tests, PVC insulated wire was used).

The voltage gain for the staged generator from stage 1 to stage 2 is about 14, effectively stepping up the voltage from 1 kV to 14 kV in the second stage. Of course, higher seed currents will lead to higher output energy and higher output voltage. As long as the wire is not excessively heated by the current flow, the energy gain and the voltage gain will exhibit only little decrease. So far, we achieved a maximum output energy of 1,500 J and an output voltage of 30 kV with the staged generator running into a $3 \mu\text{H}$ load. Figure 10 shows a current output of 15.2 kA into a $3 \mu\text{H}$ load. The initial current supplied was 2.4 kA into a $9.4 \mu\text{H}$ seed coil, L1, meaning that the overall final flux of the dual stage generator, 0.046 Wb, is twice the initial flux, 0.023 Wb, having an energy gain of ~ 13 .

Figure 11 shows the magnetic flux density distribution during the compression of the second stage when the armature reaches the helix. As this figure illustrates, the highest flux is produced at the contact point between the armature and the secondary winding where most of the intrinsic flux is lost. The magnitude of the magnetic flux density close to the secondary helix inside wall is 4 to 6 times larger at the contact point than at locations where the armature has little expanded [7].

While we have calculated the energy gain from the experiment using the final magnetic energy and the initial magnetic energy, it should be mentioned that the demand on prime energy could be considerably higher than the initial magnetic energy. Specifically, the ohmic resistance in the capacitor-inductor seed current circuit leads to non-negligible losses in the transfer from electric field energy in the capacitor to the seed current coil's magnetic field energy. Depending on the design, as much as 50 % of the initial stored energy in the capacitor is lost. As a general rule, the capacitance should be chosen as small as possible and the charging voltage as large as possible. Of

course there are limits to this as electrical breakdown between crowbar S1 and armature becomes an issue due to the voltage step-up between L1 and L2 if the charging voltage of the seed capacitor becomes too large. The use of SF_6 was needed to avoid voltage-induced breakdown when stage 2 is switched. The energy loss from CS to L1 for our staged generator was about 25 %, resulting in an effective energy gain of ~ 10 from stored energy in the capacitor to output magnetic field energy; a result that is comparable to MFCGs with somewhat larger working diameter [3].

4. Conclusion

We have presented the detailed mechanical design of a staged magnetic flux compression generator, MFCG, utilizing magnetic flux trapping. The dual stage performance as well as the performance of the single stages separately have been discussed. The 250 mm long (51 mm helix diameter) MFCG has an energy gain of 13 into a $3 \mu\text{H}$ load at an output energy of 1.5 kJ. Mostly due to the mutual inductance between the stages, the gain of the overall generator is about 30 % lower than the gain produced by the individually tested stages.

Manuscript received August 1, 2003

References

- [1] Neuber A.A., Holt T.A., Hernandez J.-C., Dickens J.C., and Magne Kristiansen Geometry Impact on Flux Losses in MCGs // Ninth Intl. Conference on Megagauss Magnetic Field Generation and Related Topics, – Moscow - St. Petersburg; – July 7–14, 2002.
- [2] Cnare E.C., Kaye R.J., and Cowan M. An Explosive Generator of Cascaded Helical Stages. Proc. of the 3rd Int. Conf. on Megagauss Magnetic Field Generation and Related Topics – Moscow, Russia: Nauka: – 1984. – P. 50–56.
- [3] Leontyev A.A., Mintsev V.B., Ushnurtsev A.Ye., Fortov V.Ye. and Shurupov A.V. Two-Stage Magnetic Flux Compressors with Flux Trapping // Proc. of the 7th Int. Conf. on Megagauss Magnetic Field Generation and Related Topics. – Sarov, Russia: – August 5–10, 1996. – P. 322–326.
- [4] Chernyshev V.K., Zharinov, E.I., Kazakov, S.A., Busin, V.N., Vaneev, V.E. and Korotkov, M.I. Magnetic flux cutoffs in helical explosive magnetic generators // Proc. of the 2nd Int. Conf. on Megagauss Magnetic Field Generation and

Related Topics. – Santa Fe, New Mexico:
– July 14–17, 1986. – P. 455–469.

- [5] Neuber A., Dickens J., Cornette J.B., Jamison K., Parkinson R., Giesselmann M., Worsley P., Baird, Schmidt M., and Kristiansen M., Electrical Behavior of a Simple Helical Flux Compression Generator for Code Benchmarking // IEEE Transactions on Plasma Science. – August 2001. – V. 29. N 4. ISSN 0093-3813. – P. 573–581.
- [6] Neuber A.A., Holt T.A., Hernandez J.-C., Dickens J.C. and Kristiansen Magne Physical Efficiency Limits of Inch-sized Helical MFCG's // presented at the 14th Pulsed Power Conference in Dallas, Texas. – June 15–18, 2003.
- [7] Neuber A.A., Thomas Holt, Juan-Carlos Hernandez, James C. Dickens, and Kristiansen M. Dependence of Flux Losses on MCG Helix Geometry // AIP Conference Proceedings. – December 17, 2002. – V. 650(1). – P. 33–36.